



## Stream Sediments Pollution Assessment in a Lead and Zinc Mining Area, Using GIS: A Case Study of the Gojer Mine, Kerman, Iran

Ali Ghorbani<sup>1</sup>, Mehdi Honarmand<sup>1\*</sup>, Mohammad Javad Hassani<sup>1</sup> and Hadi Shahriari<sup>2</sup>

<sup>1</sup> Department of Ecology, Institute of Science and High Technology and Environmental Sciences, Graduate University of Advanced Technology, Kerman, Iran, [alighorbani68414@yahoo.com](mailto:alighorbani68414@yahoo.com)

<sup>2</sup> Department of Mining Engineering, Vali-e-Asr University of Rafsanjan, Rafsanjan, Iran

Article Info	Abstract
<b>Keywords:</b> Stream Sediments pollution Heavy metals Lead- Zinc Environmental assessment Gojer mine	Lead and zinc deposits are potential sources of environmental contamination due to their high concentrations of toxic elements and heavy metals. In Kerman province, most lead and zinc mines are situated in the northern region, particularly in the Ravar area, with the Gojer lead and zinc mine being a prominent example. This study employed statistical methods such as Principal Component Analysis (PCA), Factor Analysis (FA), and environmental indices to evaluate the degree and distribution of soil and stream sediment pollution in the Gojer mine area. Statistical analysis demonstrated a strong correlation among heavy metals. Furthermore, the Enrichment Factor (EF) and Potential Ecological Risk Index (RI) indicated varying levels of heavy metal pollution in the mine area. The primary sources of contamination were identified as lead and arsenic, both of which pose significant risks to human health. The severity and spatial extent of contamination were also notable. Pollution levels were highest in close proximity to the mining site, with the presence of Gossan linked to lead and zinc mineralization. As the distance from the mining area increased, pollution levels gradually declined.

\*Corresponding author: Mehdi Honarmand

Email: [m.honarmand@kgut.ac.ir](mailto:m.honarmand@kgut.ac.ir)

<https://doi.org/10.48306/jgrs.2025.483055.1010>

Received 12 October. 2024; Received in revised form 19 October. 2024; Accepted December. 2024

Available online December 2024

©2024 Graduate University of Advanced Technology, Kerman, Iran. This is an open article under the CC BY-NC-SA 4.0 license (<https://creativecommons.org/licenses/by-nc-sa/4.0/>)

### 1. Introduction

Mining activities are a major contributor to heavy metal pollution, presenting a serious risk to the surrounding environment. Human activities, particularly mining, can adversely affect soils in the impacted regions. In older mining sites, the use of outdated and inefficient techniques often results in waste materials with elevated metal concentrations. When exposed to atmospheric conditions, these metals can be released into the soil and water systems. Soil, as a critical element of the life cycle, exhibits

diverse physical and chemical properties due to the weathering of rocks and minerals in the Earth's crust. Lead and zinc mines are particularly hazardous to the environment because of their high levels of toxic elements. Given the economic significance of mining, it is essential to conduct environmental assessments to mitigate pollution and safeguard human health. Heavy metal pollution is a worldwide issue, as these metals are chemically stable, persist in the environment, enter the food chain, and exert toxic effects on living organisms. The toxicity and bioaccumulation of heavy metals in food chains pose significant environmental and health challenges in contemporary societies. In recent years, the issue of heavy metal pollution has gained global attention owing to its persistent nature and capacity for bioaccumulation, which present serious risks to both human health and the stability of ecosystems (Islam et al., 2017) (Wang et al., 2019). Heavy metals and metalloids are recognized as among the most hazardous environmental pollutants due to their detrimental effects on soil quality, thereby undermining environmental sustainability (Islam et al., 2017). Soil, a critical natural resource essential for human survival and progress, serves as a major sink for persistent heavy metals because of its integral role in biogeochemical processes (Islam et al., 2017) (Z Chen, Y Zhao, D Chen, H Huang, Y Zhao, 2023). Unlike many other pollutants, heavy metals are not susceptible to degradation by soil organisms. Consequently, they tend to accumulate over time, leading to disruptions in the natural biogeochemical equilibrium (Z Chen, Y Zhao, D Chen, H Huang, Y Zhao, 2023)

Human activities play a significant role in contributing to environmental pollution. Research indicates that the contamination of arable land primarily stems from industrial operations, agricultural practices, and mineral extraction processes (Wang et al., 2019). Mining and related activities produce substantial amounts of waste materials containing high levels of potentially toxic elements (PTEs), such as lead (Pb), zinc (Zn), arsenic (As), and cadmium (Cd). These elements can be mobilized and transported to various environmental compartments, primarily through water runoff and wind dispersion (Ayari et al., 2023). The distribution of PTE-containing particles is influenced by numerous factors, including the properties of the ore (such as mineralogy, chemical speciation of trace elements, and waste physiochemistry), mining techniques (extraction and storage methods), and environmental conditions (climate, lithology, and topography). The presence of PTEs in environmental media poses health risks to humans and animals, primarily through contamination of the food chain and water supplies (Ayari et al., 2023)

Naturally, the concentrations of heavy metals and metalloids, such as chromium (Cr), nickel (Ni), cadmium (Cd), copper (Cu), lead (Pb), and arsenic (As), in soils are typically low, maintaining an optimal ecological balance. However, human activities often lead to elevated levels of these elements in soils. Notably, the increased concentrations of heavy metals and metalloids in agricultural soils have been widely documented and have negatively impacted numerous regions worldwide (Bou Kheir et al., 2010) (Sun et al., 2010) (ISLAM et al., 2017).

The extraction of minerals and metals has been practiced since ancient times. However, the mining industry underwent significant growth in recent centuries, becoming a crucial driver of industrial and economic progress in societies (Rashed, 2010)(Christou et al., 2017). While mining has contributed positively to human development, it has also generated vast quantities of waste, known as tailings. On average, only 1-3% of mined ore is converted into usable concentrate, leaving the remainder as waste (Adiansyah et al., 2015). Tailings consist of fine-grained, non-economic by-products containing trace amounts of valuable minerals or metals, acidic materials rich in sulfides and sulfates, heavy metals, organic compounds, and processed water. These materials are often deposited untreated, forming tailing dams or large spoil heaps that occupy significant land areas globally (Christou et al., 2017) Active and, more commonly, abandoned mine tailings are frequently left unmanaged or improperly managed, making them unstable and susceptible to erosion by wind and water. Additionally, they are prone to producing acid mine drainage, which exacerbates environmental degradation (Christou et al., 2017). Lead and zinc deposits, in particular, pose a significant risk of environmental contamination due to their high concentrations of toxic elements and heavy metals.

During the 19th and early 20th centuries, zinc production predominantly relied on smithsonite-bearing "oxide" (non-sulfide) ores, which were processed using Wälz kilns. However, with the advent of differential flotation techniques and advancements in smelting and refining sphalerite concentrates in the early 20th century, sulfide ores became the primary source of zinc production. The metallurgical challenges associated with processing smithsonite ores, which typically contained 10 to 20 percent zinc along with zinc oxide, silicates, and clays, led to the neglect of large deposits of non-sulfide zinc materials as viable sources of zinc. In recent years, the development of hydrometallurgical methods, including acid-leaching, solvent extraction, and electrowinning, has revived commercial interest in non-sulfide zinc deposits as a significant potential source of zinc for the 21st century (Hitzman et al., 2003). Zinc deposits are generally classified into two main types: supergene and hypogene deposits(Hitzman et al., 2003). In Iran, notable non-sulfide zinc mines include Angouran, Mehdi-Abad, Iran-Kuh, and Kuh-e-Surmeh, which have been recognized for their economic potential (Reichert and Borg, 2008)(Maghfouri et al., 2018). Most of Kerman's lead and zinc mines are located in the north of the province in the Ravar area, among them, Gojer's lead and zinc mine can be mentioned that have long been under exploration and extraction operations. Due to long activities and of course, low environmental standards, areas of this kind of deposits are susceptible to environmental pollution. Therefore, the degree and distribution of soil and stream sediment pollution in the Gojer mine area were investigated through Geostatistics and geochemical parameters.

## **2. Study area**

Gojer's Zinc mine is one of the most important zinc and non-sulfide mines in Kerman province. The study area is located in the central tectonic zone of Iran (Fig.1 A) and the southeast corner of the

1/100000 scale geological map of Bahabad (Fig.1 B). The Gojer mine has two eastern and western anomalies in which western anomalies have been extracted in the past and mining activity continued, but the eastern anomaly has been explored and has not been mined as yet. Based on local and detailed geological research these rocks belong to the Devonian Carboniferous and the Lower to Middle Triassic. In general, according to the geological map of 1/5000 (Fig 1C), the main units located in the Gojer mineral District are broadly carbonate units such as limestone, dolomite, dolomitic limestone, limestone, and silty dolomite. Other rock units in the area of the Gojer mine are red sandstones, shale, and evaporative.

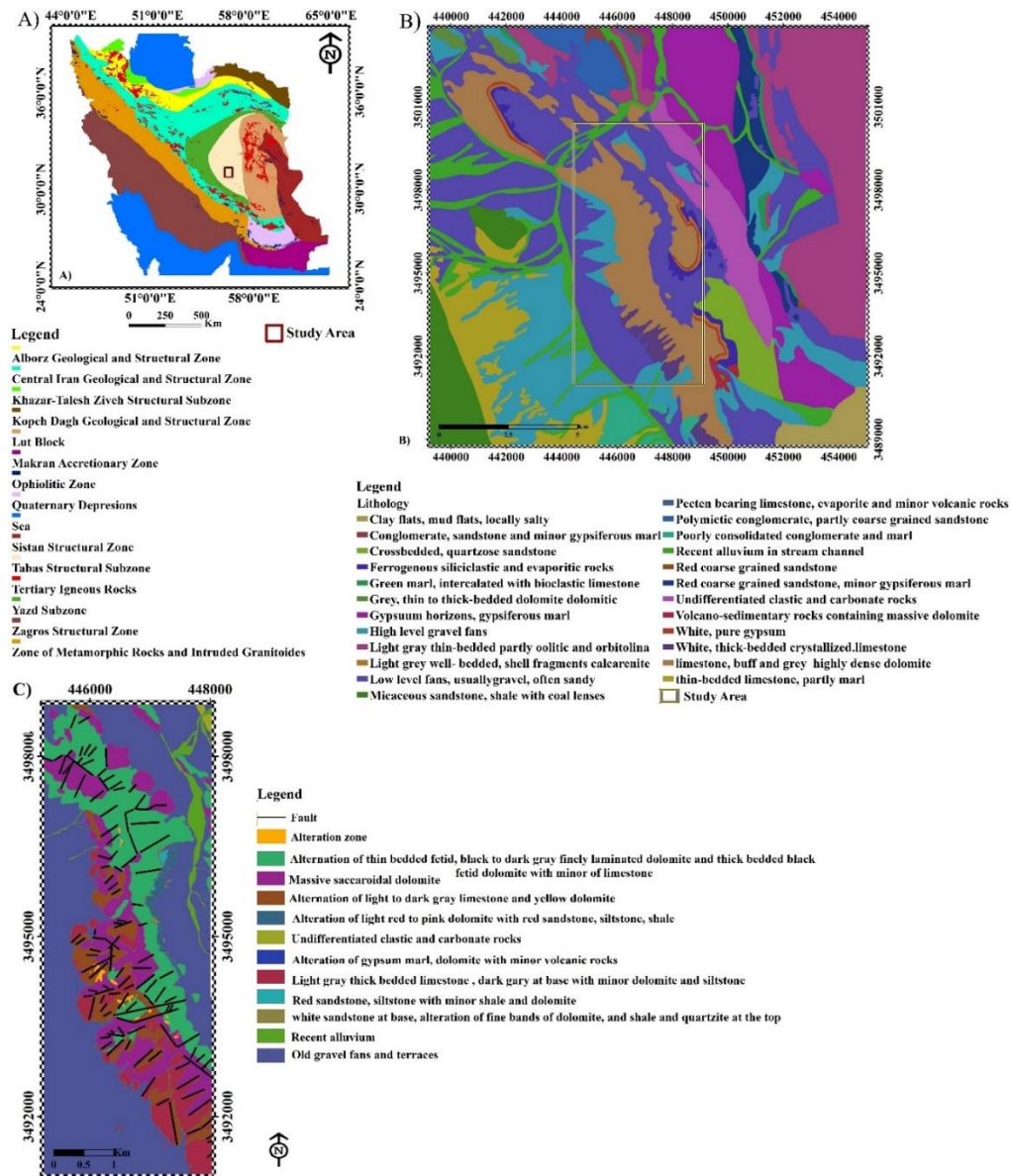


**Figure-1.** A) Location of the study area in the Iran's structural zones, B) The geological map of the area that is extracted from the southeastern part of the 1/100000 Bahabad geological sheet and the area of the Gojer mine is shown by the yellow square, C) Geological map on the scale of 1/ 5000 for Gojer mine.

### 3. Material and methods

In this research, geostatistical and geochemical parameters are used to demonstrate the dispersion of toxic elements in stream sediments within the Gojer mine area. The study utilizes 41 sediment samples collected from streams draining the mine. Additionally, Geographic Information Systems (GIS) were employed to visually represent and map the findings. GIS serves as a robust tool for spatial data visualization, significantly contributing to the analysis and interpretation of geochemical contamination. By overlaying point data from factor analysis and soil contamination indices onto maps, GIS facilitates the identification of spatial patterns in pollution distribution. This functionality enables the pinpointing of regions with the highest contaminant concentrations and the exploration of relationships between pollution and other environmental variables. Furthermore, GIS can be used to evaluate contamination risk and prioritize areas for remediation efforts. The generation of diverse maps, including point maps, provides a visual and comprehensible means of conveying complex information, thereby aiding in informed management decisions.

**Statistical analyses:** Analysis of variance (ANOVA) was conducted to assess significant spatial and temporal variations. The relationships between different elements in soil samples were evaluated using the non-parametric Spearman rank correlation method. Multivariate analysis of stream sediment data was performed through cluster analysis (CA), which groups sampling sites based on similarities in heavy metal concentrations within bioavailable fractions. CA was utilized to identify distinct geochemical groups by clustering samples with comparable heavy metal contents. Principal Component Analysis (PCA) was employed to deduce potential sources of heavy metals, distinguishing between natural and anthropogenic origins. Factor Analysis (FA), derived from PCA components, was conducted using Varimax rotation. This orthogonal rotation method was chosen as it reduces the number of variables with high loadings on each component, thereby simplifying the interpretation of PCA results (Bhuiyan et al., 2010). To ensure accuracy and avoid misclassification caused by variations in data dimensionality, the experimental data were standardized using z-scale transformation before applying the statistical analyses. The suitability of the data for PCA/FA was evaluated using the Kaiser–Meyer–Olkin (KMO) measure of sampling adequacy and Bartlett’s sphericity test. The KMO statistic quantifies the proportion of common variance, which may be attributed to underlying factors. A KMO value close to 1 suggests that PCA/FA is appropriate for the dataset (Varol, 2011). The KMO index ranges from 0 to 1, with values exceeding 0.7 indicating that the data are highly suitable for factor analysis.

**Enrichment factor (EF):** A widely used method to assess anthropogenic influence on sediment composition involves calculating a normalized enrichment factor (EF) for metal concentrations relative to uncontaminated background levels (Salomons and Förstner, 1984). The EF approach aims to minimize variability in metal concentrations caused by differences in mud-to-sand ratios, making it a practical tool for identifying geochemical trends across extensive geographic regions with significant variations in sediment composition, particularly the proportion of clay-rich mud to sand (Abraham and Parker, 2008).

The EF method normalizes the measured concentrations of heavy metals using a reference metal, such as iron (Fe) or aluminum (Al) (Ravichandran et al., 1995). Fe has been proposed as a suitable normalization element for EF calculations, as its distribution is generally independent of other heavy metals (Deely and Fergusson, 1994). Additionally, Fe typically occurs at relatively high natural concentrations in sediments, making it less likely to be significantly enriched by anthropogenic activities in estuarine environments (Niencheski and Baumgarten, 2000). The enrichment factor (EF) is calculated using the following formula:

$$EF = \frac{[C_x/C_{ref}]_{Sample}}{[B_x/B_{ref}]_{Background}}$$

Where:  $C_x$  = concentration of the target element in the examined environment (e.g., samples from surrounding areas or stream sediments);  $C_{ref}$  = concentration of the target element in the reference environment (e.g., the Earth's crust, based on Clark concentrations);  $B_x$  = concentration of the reference element in the examined environment; and  $B_{ref}$  = concentration of the reference element in the reference environment (e.g., the Earth's crust, based on Clark concentrations) (Addo et al., 2012).

A suitable reference element must meet specific criteria, including: (I) high natural abundance in sediments, (II) minimal influence from anthropogenic sources, (III) ease of measurement using analytical techniques, and (IV) resistance to contamination during sampling. Commonly used reference elements include aluminum (Al) and iron (Fe) (Yuan et al., 2017)(Chabukdhara and Nema, 2012). In this study, Fe was selected as a conservative tracer to distinguish between natural and anthropogenic contributions. The classification of enrichment factors is presented in Table 1..

**Table-1.** Enrichment Factor Classes (Chen et al., 2007)

EF	Enrichment Factor Classes
$\leq 1$	indicates no enrichment
1-3	is minor enrichment
3-5	is moderate enrichment
5-10	is moderately severe enrichment
10-25	is severe enrichment
25-50	is very severe enrichment
$\geq 50$	is extremely severe enrichment

**Risk assessment:** Heavy metals in sediments are distributed across various fractions with differing binding strengths, which directly influences their presence and mobility in associated aquatic environments (Sundaray et al., 2011). The extent of risk associated with these fractions can be quantified and managed through risk assessment methodologies (Li et al., 2007). Risk assessment evaluates the bioavailability of heavy metals in sediments by assessing the proportion of metals present in

exchangeable and carbonate fractions, which are more likely to be released into the environment (Singh et al., 2005)(Sundaray et al., 2011). To quantitatively assess the potential pollution levels of heavy metals, the Hakanson pollution assessment method was employed. This approach, introduced by Hakanson in 1980, is based on the toxicity levels of heavy metals and has been widely utilized for evaluating heavy metal pollution risks. The method provides a systematic framework for assessing contamination, and its principles are detailed in the referenced studies (Hakanson, 1980)(Chen et al., 2017) and the formula is as follows:

$$C_f^i = \frac{C_n^i}{C_0^i}$$

$$E_r^i = T_r^i \times C_f^i$$

$$RI = \sum_{i=1}^n E_r^i$$

Risk Assessment Methodology: The Risk Index (RI) represents the cumulative potential risk of multiple heavy metals, calculated as the sum of individual risks  $E_r^i$  for each metal. The individual risk  $E_r^i$  is determined by multiplying the contamination coefficient  $C_f^i$  by the toxic-response factor  $T_r^i$  for the specific heavy metal. The contamination coefficient  $C_f^i$  is derived by dividing the current concentration of the heavy metal in sediments  $C_n^i$  by its pre-industrial background concentration  $C_0^i$  (Hakanson, 1980)(Zhu et al., 2012)(Chen et al., 2017).

The toxicity levels of heavy metals follow this order: Zn = 1, Cr = 2, Cu = 5, Pb = 5, Ni = 5, As = 10, and Cd = 30 (Islam et al., 2017)(Hakanson, 1980)(Mirzaei et al., 2014)(Chen et al., 2017)(Zhu et al., 2012)

For ecological risk assessment,  $E_r^i$  is categorized into 5 classes, while RI is divided into 4 classes, as outlined in the table below (Hakanson, 1980)(Krupadam, Smita and Wate, 2006) . Table 2 provides a detailed description and classification of ecological risk values.

**Table-2.**Indices and ranks of potential ecological metals contamination (Zhu et al., 2012)

Grade of potential ecological risk of environment	RI	Grade of ecological risk of single-metal	ER
Low risk	<b>RI&lt;150</b>	Low risk	<b><math>E_r^i &lt; 40</math></b>
Moderate risk	<b>150 ≤ RI &lt; 300</b>	Moderate risk	<b>40 ≤ <math>E_r^i</math> &lt; 80</b>
Considerable risk	<b>300 ≤ RI &lt; 600</b>	Considerable risk	<b>80 ≤ <math>E_r^i</math> &lt; 160</b>
Very high risk	<b>RI ≥ 600</b>	High risk	<b>160 ≤ <math>E_r^i</math> &lt; 320</b>
		Very high risk	<b><math>E_r^i \geq 320</math></b>

## 4. Results and Discussion

Alluvial sediments have long been used in geochemical surveys as their compositions are assumed to be representative of areas upstream (Lipp, de Caritat and Roberts, 2023). Each variable within the stream sediments possesses a vector property, representing its upstream values. Consequently, due to the directional nature of this data, reflecting changes in the upstream basins, the presence of anomalies in these sediments indicates the existence of an upstream source. In weathered environments, many minerals, particularly sulfur-bearing species, are unstable and decompose through oxidation and other chemical reactions. This process leads to the dispersion of elements and can result in environmental contamination. Human activities, such as mining, significantly contribute to and exacerbate this contamination. Understanding the extent and distribution of pollution within the environment is crucial.

### **Statistical Analysis of Geochemical Data:**

Prior to any analysis or processing of raw geochemical data, it is essential to determine the statistical properties and distribution function of the data. To achieve this, statistical parameters such as average, mean, standard deviation, skewness, kurtosis, and minimum and maximum values were calculated. Additionally, histograms were generated for all elements to assess their distribution patterns. For data normalization, a simple logarithmic or three-parameter method can be employed. It is important to note that normalization does not eliminate geochemical anomalies. In this research, a simple logarithmic method was utilized to normalize the data.

### **Factor Analysis: Interpreting Geochemical Data**

The Kaiser-Meyer-Olkin (KMO) index for the Gojer mine data was 0.789, indicating that the data are suitable for factor analysis. To improve the interpretability of the factors without altering the total variance, a varimax rotation was applied. Table 3 presents the factor loadings derived from the rotated factorial data analysis of the study area. Figure 2 depicts the relative dispersion diagram of the elements used in this analysis in the rotated space. The absolute magnitude of these factor loadings indicates the relative importance of each factor in explaining the overall variation of the corresponding variable. Factor analysis identified three factors related to the elements in this study. The first factor comprises arsenic, silver, copper, and molybdenum. Examining the second component, iron (Fe) and manganese (Mn) exhibit high factor loadings. This indicates a strong correlation between these two elements, suggesting enrichment through a similar geochemical process. Iron and manganese typically precipitate as insoluble oxides in oxidizing environments. Given their similar geochemical properties, including ease of oxidation and formation of insoluble hydroxides, these elements often co-precipitate in oxidizing environments. To investigate the association between lead (Pb) and zinc (Zn), we examine components where both elements exhibit significant factor loadings. In this matrix, the third component appears to have high factor loadings for both lead and zinc. A strong correlation between lead and zinc is often attributed to anthropogenic sources. While lead and zinc can occur naturally in sulfide minerals and be released during mining activities, the high zinc concentration in this dataset, which is from a zinc mine,

suggests that the high factor loading for zinc in the third component may simply reflect the element's intrinsic abundance in the study area. If lead and zinc exhibit high factor loadings on a common component, it indicates that these two elements are involved in a shared geological or pollution process. This could signify a genetic association between these elements or input from a common pollution source. According to Table 4, the first three factors explain 67.511%, 13.919%, and 12.177% of the total variance, respectively. In total, these factors account for over 93% of the variables' information. This suggests that the first, second, and third factors represent the highest levels of heavy metal pollution in the region.

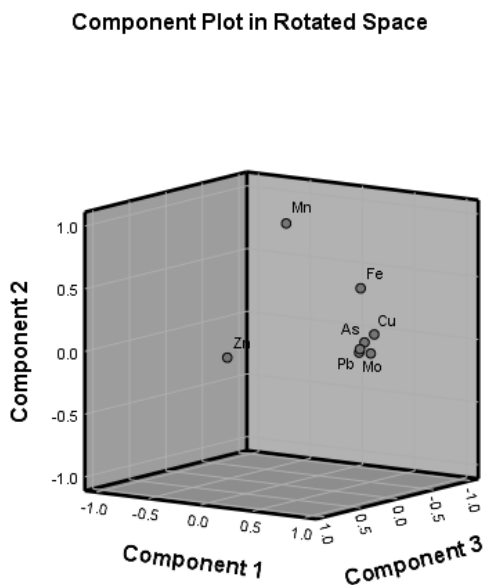


**Figure-2.** Dispersion pattern of elements in the evolved environment in the analysis of the factor of the Gojer mine.

**Table-3.** Matrix of the rotated components in the analysis of the factor of the Gojer mine.

	Rotated Component Matrix							
	Component							
	1	2	3	4	5	6	7	8
Zn	.167	.062	.984	.018	-.003	-.001	.003	.002
Pb	.938	.103	.266	.110	-.032	-.006	-.024	.156
Mo	.768	.025	.034	.637	.048	.014	.006	.003
Mn	.095	.993	.073	.008	.016	.007	.004	.002
Fe	.732	.524	-.038	.130	.412	.031	.011	-.005
Cu	.918	.187	.041	.166	.172	.251	.002	-.016
As	.917	.142	.173	.251	.068	.028	.199	-.009
Ag	.959	.053	.147	.054	.022	-.171	-.108	-.110

**Table-4.** Total variance of each of the components of factor analysis in Gojer mine.

<b>Total Variance Explained</b>									
Component	Initial Eigenvalues			Extraction Sums of Squared Loadings			Rotation Sums of Squared Loadings		
	Total	% of Variance	Cumulative %	Total	% of Variance	Cumulative %	Total	% of Variance	Cumulative %
1	5.401	67.511	67.511	5.401	67.511	67.511	4.647	58.087	58.087
2	1.114	13.919	81.431	1.114	13.919	81.431	1.333	16.661	74.748
3	.974	12.177	93.608	.974	12.177	93.608	1.100	13.750	88.498
4	.239	2.985	96.593	.239	2.985	96.593	.529	6.607	95.105
5	.131	1.638	98.231	.131	1.638	98.231	.208	2.601	97.706
6	.076	.953	99.184	.076	.953	99.184	.094	1.181	98.887
7	.038	.476	99.660	.038	.476	99.660	.052	.652	99.539
8	.027	.340	100.000	.027	.340	100.000	.037	.461	100.000

### Enrichment Factor Analysis

The enrichment factors (EFs) for heavy metals and toxic elements (manganese, lead, zinc, molybdenum, and arsenic) were calculated within the Gojer mine area. Figure 3 illustrates the dispersion map for the enrichment factors of arsenic, molybdenum, lead, zinc, copper, and manganese. Copper exhibits relatively strong enrichment at two points near the eastern anomaly and three points with a moderate degree near the western anomaly. Manganese demonstrates consistently severe enrichment, while lead shows extreme enrichment throughout the study area. Molybdenum exhibits two points of severe enrichment at the eastern anomaly and one point at the western anomaly; Additionally, five points of moderate enrichment are observed at the western anomaly, while one point at the eastern anomaly and other stations show little or no enrichment. Arsenic and zinc exhibit very severe to extreme enrichment at both anomalies, particularly zinc. In areas distant from the mine's activities, both elements show low enrichment. In most cases, very high concentrations (very severe to very extreme) of contamination coincide with areas close to the east and west anomalies. As the distance from these anomalies increases, contamination levels generally decrease, except for lead, which consistently exhibits extreme enrichment at all stations.

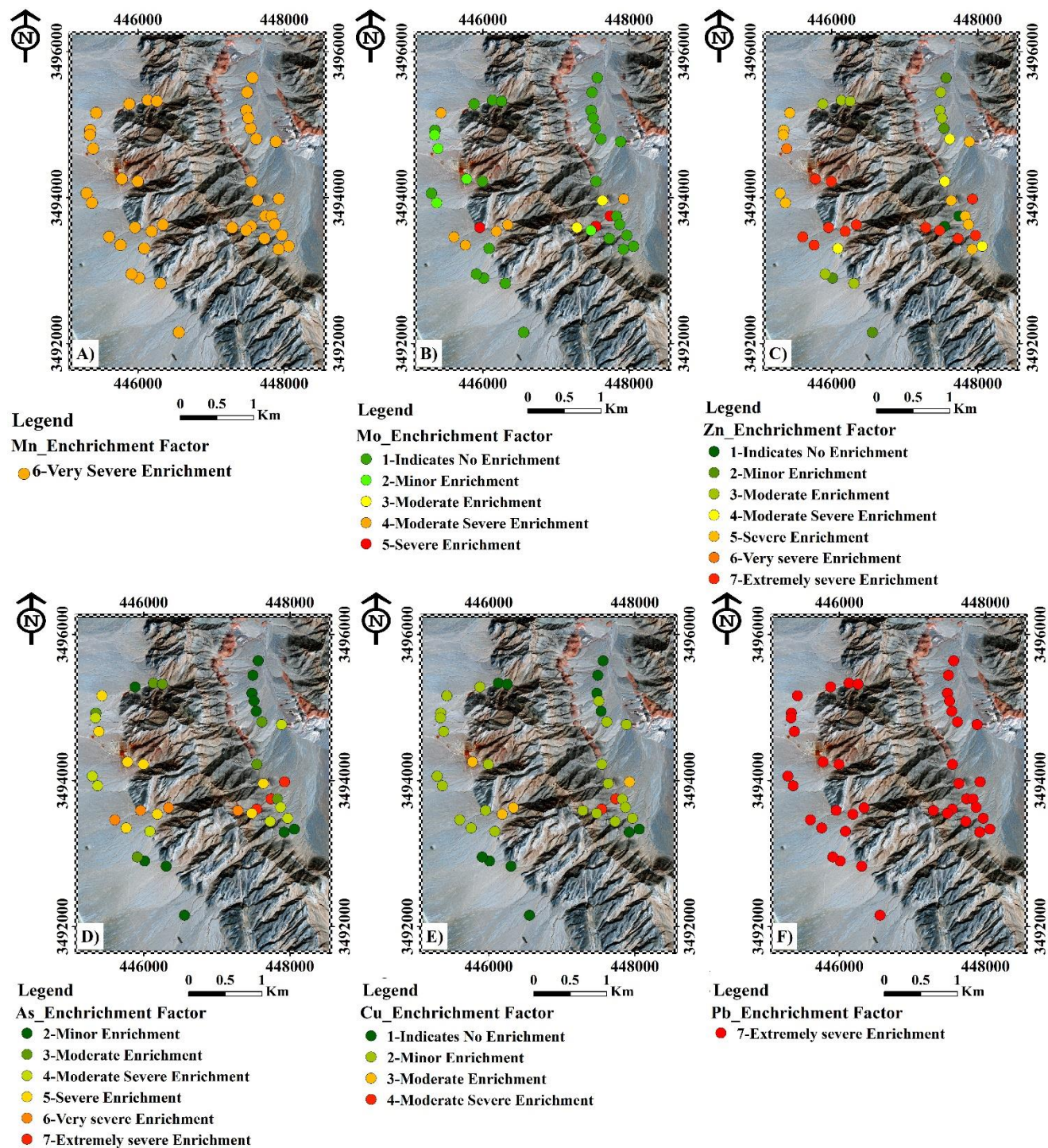


**Figure-3.** Enrichment Factor map for each Element and Enrichment Factor for Gojer Mine, A) Manganese enrichment factor that determines the concentration of pollution in mining areas, B) molybdenum enrichment factor that shows moderate to relatively severe enrichment in the mining activity area, C) Zinc enrichment factor that shows a high to severe contamination rate in mining areas, D) arsenic enrichment factor that shows a high to severe contamination rate in mining areas, E) copper enrichment factor that shows extreme enrichment in mining activity areas, and the greater the distance from mining activity area, the amount of enrichment is reduced, F) Lead Enrichment Factor which at all locations shows "extremely severe enrichment".

### **Potential Ecological Risk Assessment**

The potential ecological risk (PER) associated with heavy metals and toxic elements (copper, lead, zinc, and arsenic) was calculated using an ecological risk index within the Gojer mine area. Figure 4 illustrates the PER maps for these elements. Copper was found to pose no ecological risk. Arsenic, even at levels below the ecological risk threshold, presents ecological risks, particularly in the eastern anomaly where the risk is very high. As distance from the mining site increases, the ecological risk of arsenic decreases. Zinc exhibits no ecological risk in most areas, with moderate to high risks only observed in the vicinity of the eastern and western anomalies, the primary sources of mining activity. Lead poses severe to very severe ecological risks in many areas, especially within the mining region. However, the ecological risk of lead decreases with increasing distance from the mine's activities, eventually reaching low levels. Figure 6 depicts the ecological risk index (RI) map for the Gojer Mine. Areas close to mining activity exhibit very high RIs, even reaching high levels. Conversely, areas with lower ecological risks are located further away from mining activities, with a decreasing RI as distance increases. Figure 5 illustrates the dispersion map for the RIs of lead, zinc, copper, and arsenic. Among the elements examined, copper was found to pose no ecological risk. Zinc exhibits significant ecological risk only at three points near the anomalies, with moderate to low risks elsewhere. Arsenic and lead, on the other hand, present very high ecological risks, especially within the anomalies. Figure 7 also demonstrates that the RI is very high in areas close to the east and west anomalies, with a decreasing RI as the distance from the anomalies increases.

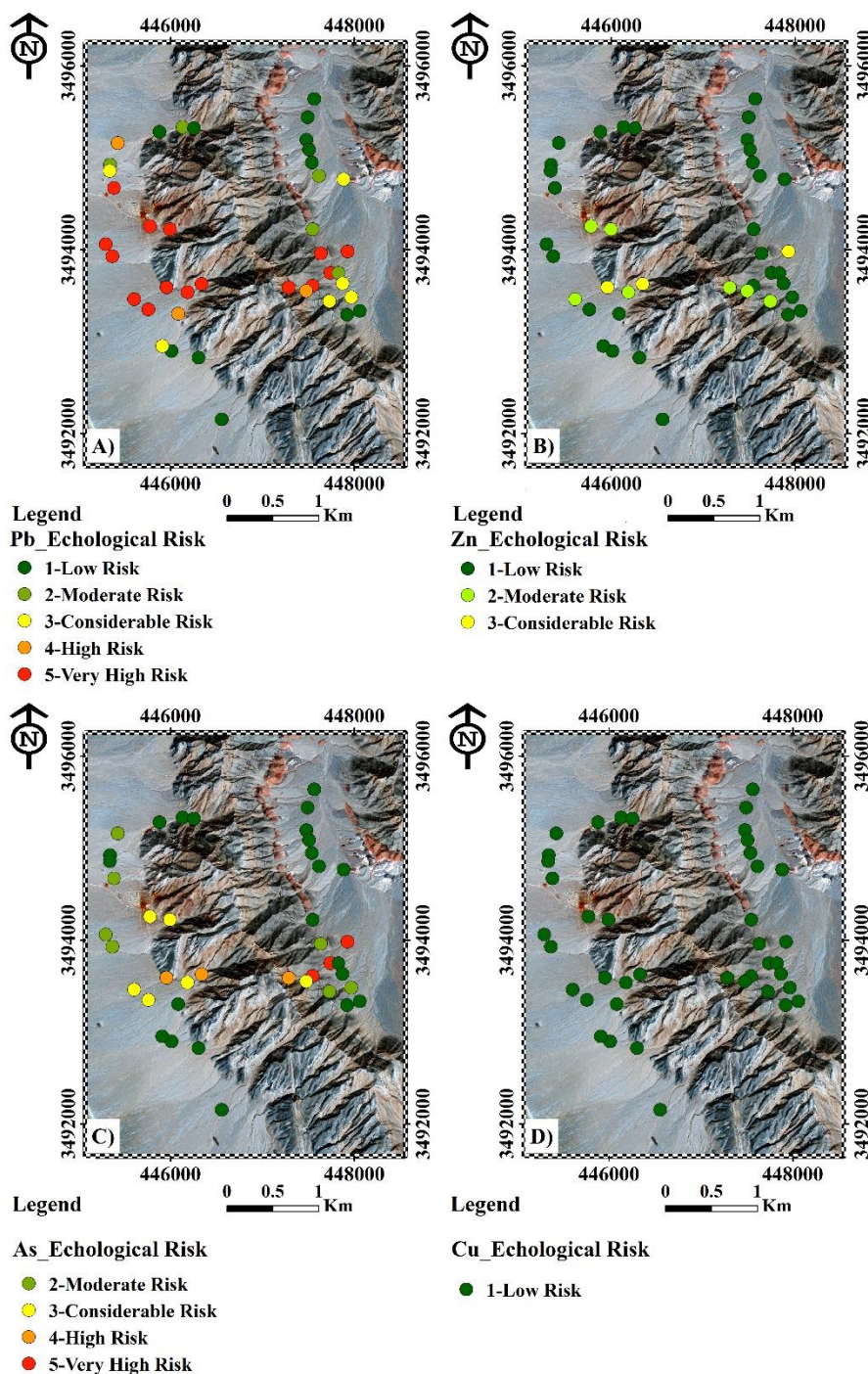


**Figure-4.** Ecologic Risk Potential Distribution map for each Element and Ecological Risk Index in Gojer Mine.

A) Ecologic Risk Potential Distribution map of lead that in most places shows a severe to very severe ecological risk that is consistent with mining areas. B) Dispersion map of the Zinc Ecological Risk Potential which has a medium to high risk in the places near the mining activity. C) Ecologic Risk Potential Distribution Map of Arsenic that has been Ecologically Risky in Mining Areas Especially in the East Anomaly which has a very high risk, and its ecological risk is reduced as it moves away from the mining site. D) Dispersion map of the Copper Ecological Risk Potential which has a low risk in all places.

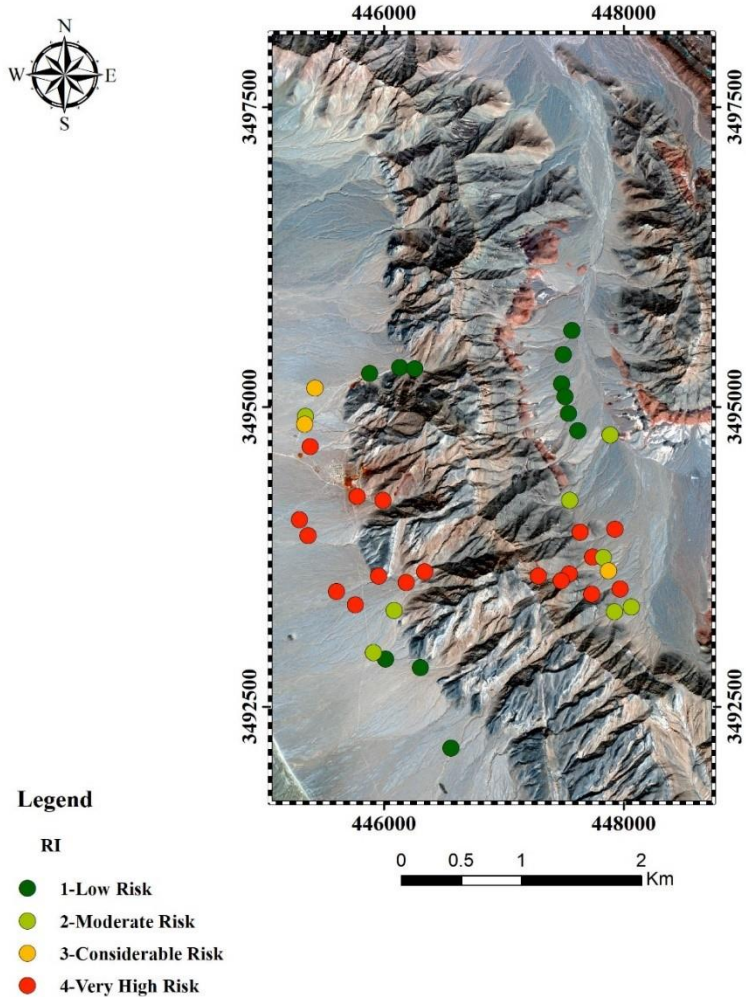


**Figure-5.** The Distribution map of the Ecological Risk Index of Gojer mine is very high at locations close to the mining activity area and they are even at very high risk in terms of ecological risk index, and less risky points are those that are far from mining activity. As the distance becomes greater the risk becomes lower in such a way that it reaches low risk values.

This study investigated the geochemical distribution of heavy metals in stream sediments near the Gojer Mine. The results demonstrate the significant impact of mining activities on the surrounding environment, particularly in terms of heavy metal contamination. Factor analysis revealed three principal factors controlling the distribution of elements. The first factor, characterized by high loadings of arsenic, silver, copper, and molybdenum likely reflects the influence of the mine's primary ore mineralization and associated geochemical processes. The second factor, dominated by manganese and Iron, may indicate the influence of weathering processes or secondary mineral formation. The third factor,

primarily driven by zinc and lead, likely reflects the high abundance of zinc within the mine's ore body. Enrichment factor analysis confirmed the significant enrichment of various heavy metals, particularly lead, arsenic, manganese, and zinc, in the vicinity of the mine. The spatial distribution of enrichment factors indicates that the anomalies are associated with the mine's activities, suggesting that mining operations have released these elements into the environment. The ecological risk assessment revealed that lead and arsenic pose the most significant ecological risks. High ecological risk values were observed in areas close to the mine, emphasizing the detrimental impact of mining on the surrounding ecosystem. While zinc showed moderate ecological risk in some areas, copper was found to pose negligible ecological risk. The observed spatial patterns of contamination, with higher concentrations closer to the mine and decreasing levels with increasing distance, are consistent with the expected dispersal of contaminants from the mine site. This suggests that the mine's activities have significantly impacted the surrounding environment, leading to the release of heavy metals into the stream sediments and subsequent contamination of the ecosystem.

## **5. Conclusion**

Statistical analyses reveal a strong correlation among heavy metals and toxic elements within the Gojer mine area, indicating significant contamination. Enrichment factor analysis reveals low to moderate enrichment for copper. Other elements, particularly lead, zinc, and arsenic, exhibit varying degrees of enrichment, with strong enrichment observed at most mining points. Individual ecological risk assessments indicate that copper poses a low risk within the mining area and sampling points. However, other elements, including lead and arsenic, exhibit a range of risks from low to very high. The majority of the ecological risk is associated with lead and arsenic, particularly in stations close to mining activities. The ecological risk index results further support the presence of high ecological risks at mining stations. As distance from the anomalies and mining area increases, the ecological risk decreases, eventually reaching low levels. The statistical analyses and contamination indices demonstrate that the Gojer mine is contaminated with heavy metals and toxic elements. The dispersion of contamination is consistent with the areas where mining activities are conducted. The extent and severity of pollution decrease as distance from the mining site increases. Lead and arsenic, which are harmful to human health, are the primary contaminants. These metals exhibit severe and high levels of contamination. The findings suggest that zinc and lead mines in the Ravar region have a significant negative impact on the surrounding environment due to mining activities

## 6. References

1. Abraham, G.M.S. and Parker, R.J. (2008) 'Assessment of heavy metal enrichment factors and the degree of contamination in marine sediments from Tamaki Estuary , Auckland , New Zealand', *Environmental monitoring and assessment*, 136, pp. 227–238. Available at: <https://doi.org/10.1007/s10661-007-9678-2>.
2. Addo, M.A. et al. (2012) 'Heavy Metal Concentrations in Road Deposited Dust at Ketu-South', *International Journal of Science and Technology*, 2(1), pp. 28–39.
3. Adiansyah, J.S. et al. (2015) 'A framework for a sustainable approach to mine tailings management: Disposal strategies', *Journal of Cleaner Production*, 108, pp. 1–13. Available at: <https://doi.org/10.1016/j.jclepro.2015.07.139>.
4. Ayari, J. et al. (2023) 'Trace metal element pollution in media from the abandoned Pb and Zn mine of Lakhout, Northern Tunisia', *Journal of Geochemical Exploration*, 247(November 2022), p. 107180. Available at: <https://doi.org/10.1016/j.gexplo.2023.107180>.
5. Bhuiyan, M.A.H. et al. (2010) 'Heavy metal pollution of coal mine-affected agricultural soils in the northern part of Bangladesh', 173, pp. 384–392. Available at: <https://doi.org/10.1016/j.jhazmat.2009.08.085>.
6. Bou Kheir, R. et al. (2010) 'Spatial soil zinc content distribution from terrain parameters: A GIS-based decision-tree model in Lebanon', *Environmental Pollution*, 158(2), pp. 520–528. Available at: <https://doi.org/10.1016/j.envpol.2009.08.009>.
7. Chabukdhara, M. and Nema, A.K. (2012) 'Chemosphere Assessment of heavy metal contamination in Hindon River sediments : A chemometric and geochemical approach', *Chemosphere*, 87(8), pp. 945–953. Available at: <https://doi.org/10.1016/j.chemosphere.2012.01.055>.
8. Chen, C.W. et al. (2007) 'Distribution and accumulation of heavy metals in the sediments of Kaohsiung Harbor, Taiwan', *Chemosphere*, 66(8), pp. 1431–1440. Available at: <https://doi.org/10.1016/j.chemosphere.2006.09.030>.
9. Chen, Y. et al. (2017) 'Spatial characteristics of heavy metal pollution and the potential ecological risk of a typical mining area : A case study in China', *Process Safety and Environmental Protection* [Preprint]. Available at: <https://doi.org/10.1016/j.psep.2017.10.008>.
10. Christou, A. et al. (2017) 'Assessment of toxic heavy metals concentrations in soils and wild and cultivated plant species in Limni abandoned copper mining site, Cyprus', *Journal of Geochemical Exploration*, 178, pp. 16–22. Available at: <https://doi.org/10.1016/j.gexplo.2017.03.012>.
11. Deely, J.M. and Fergusson, J.E. (1994) 'Heavy metal and organic matter concentrations and distributions in dated sediments of a small estuary adjacent to a small urban area', *Science of the Total Environment*, 153, pp. 97–111.
12. Hakanson, L. (1980) 'AN ECOLOGICAL RISK INDEX FOR AQUATIC POLLUTION CONTROL. A SEDIMENTOLOGICAL APPROACH', *Water Research*, 14(8), pp. 975–1001. Available at: [https://doi.org/10.1016/0043-1354\(80\)90143-8](https://doi.org/10.1016/0043-1354(80)90143-8).
13. Hitzman, M.W. et al. (2003) 'Classification, genesis, and exploration guides for nonsulfide zinc deposits',

- Economic Geology, 98(4), pp. 685–714. Available at: <https://doi.org/10.2113/gsecongeo.98.4.685>.
14. Islam, M.S. et al. (2017) ‘Heavy metals in the industrial sludge and their ecological risk: A case study for a developing country’, *Journal of Geochemical Exploration*, 172, pp. 41–49. Available at: <https://doi.org/10.1016/j.gexplo.2016.09.006>.
  15. ISLAM, M.S. et al. (2017) ‘Sources and Ecological Risk of Heavy Metals in Soils of Different Land Uses in Bangladesh’, *Pedosphere*, 0160(17). Available at: [https://doi.org/10.1016/S1002-0160\(17\)60394-1](https://doi.org/10.1016/S1002-0160(17)60394-1).
  16. Krupadam, R.J., Smita, P. and Wate, S.R. (2006) ‘Geochemical fractionation of heavy metals in sediments of the Tapi estuary’, *Geochemical Journal*, 40(5), pp. 513–522. Available at: <https://doi.org/10.2343/geochemj.40.513>.
  17. Li, R. et al. (2007) ‘Fractionation of Heavy Metals in Sediments from Dianchi’, *Pedosphere*, 17(2005406711), pp. 265–272.
  18. Lipp, A.G., de Caritat, P. and Roberts, G.G. (2023) ‘Geochemical mapping by unmixing alluvial sediments: An example from northern Australia’, *Journal of Geochemical Exploration*, 248(January), p. 107174. Available at: <https://doi.org/10.1016/j.gexplo.2023.107174>.
  19. Maghfouri, S. et al. (2018) ‘A review of major non-sulfide zinc deposits in Iran’, *Geoscience Frontiers*, 9(1), pp. 249–272. Available at: <https://doi.org/10.1016/j.gsf.2017.04.003>.
  20. Mirzaei, R. et al. (2014) ‘Ecological risk of heavy metal hotspots in topsoils in the Province of Golestan, Iran’, *Journal of Geochemical Exploration*, 147(PB), pp. 268–276. Available at: <https://doi.org/10.1016/j.gexplo.2014.06.011>.
  21. Niencheski, L.F. and Baumgarten, M.G.Z. (2000) ‘Distribution of particulate trace metal in souther part of the Patos Lagoon estuary’, *Aquatic Ecosystem Health and Management*, 3(2), pp. 515–520.
  22. Rashed, M.N. (2010) ‘Monitoring of contaminated toxic and heavy metals, from mine tailings through age accumulation, in soil and some wild plants at Southeast Egypt’, *Journal of Hazardous Materials*, 178, pp. 739–746.
  23. Ravichandran, M. et al. (1995) ‘History of trace metal pollution in Sabine-Neches estuary, Beaumont, Texas’, *Environmental science & technology*, 29(6), pp. 1495–1503.
  24. Reichert, J. and Borg, G. (2008) ‘Numerical simulation and a geochemical model of supergene carbonate-hosted non-sulphide zinc deposits’, 33, pp. 134–151. Available at: <https://doi.org/10.1016/j.oregeorev.2007.02.006>.
  25. Salomons, W. and Förstner, U. (1984) *Metals in the Hydrocycle*. Springer Berlin Heidelberg.
  26. Singh, K.P. et al. (2005) ‘Studies on distribution and fractionation of heavy metals in Gomti river sediments - A tributary of the Ganges, India’, *Journal of Hydrology*, 312(1–4), pp. 14–27. Available at: <https://doi.org/10.1016/j.jhydrol.2005.01.021>.
  27. Sun, Y. et al. (2010) ‘Spatial, sources and risk assessment of heavy metal contamination of urban soils in typical regions of Shenyang, China’, *Journal of Hazardous Materials*, 174(1–3), pp. 455–462. Available at: <https://doi.org/10.1016/j.jhazmat.2009.09.074>.

28. Sundaray, S.K. et al. (2011) 'Geochemical speciation and risk assessment of heavy metals in the river estuarine sediments-A case study: Mahanadi basin, India', *Journal of Hazardous Materials*, 186(2–3), pp. 1837–1846. Available at: <https://doi.org/10.1016/j.jhazmat.2010.12.081>.
29. Varol, M. (2011) 'Assessment of heavy metal contamination in sediments of the Tigris River (Turkey) using pollution indices and multivariate statistical techniques', *Journal of Hazardous Materials*, 195, pp. 355–364. Available at: <https://doi.org/10.1016/j.jhazmat.2011.08.051>.
30. Wang, N. et al. (2019) 'Potential ecological risk and health risk assessment of heavy metals and metalloids in soil around Xunyang mining areas', *Sustainability*, 11(18), p. 4828.
31. Yuan, Y. et al. (2017) 'Geochemical characteristics of heavy metal contamination induced by a sudden wastewater discharge from a smelter', *Journal of Geochemical Exploration*, 176, pp. 33–41. Available at: <https://doi.org/10.1016/j.gexplo.2016.07.005>.
32. Z Chen, Y Zhao, D Chen, H Huang, Y Zhao, Y.W. (2023) 'Ecological risk assessment and early warning of heavy metal cumulation in the soils near the Luanchuan molybdenum polymetallic mine concentration area', *China Geology*, 6(1), pp. 15–26. Available at: <https://doi.org/10.31035/cg2023003>.
33. Zhu, H.N. et al. (2012) 'Ecological risk assessment of heavy metals in sediments of Xiawan Port based on modified potential ecological risk index', *Transactions of Nonferrous Metals Society of China (English Edition)*, 22(6), pp. 1470–1477. Available at: [https://doi.org/10.1016/S1003-6326\(11\)61343-5](https://doi.org/10.1016/S1003-6326(11)61343-5).